The seismic behaviour of reinforced concrete structural walls: Experiments and modelling

Panagiotis Kotronis, J. Mazars, Xuân-Huy Nguyen, Nicolae Ile, Jean-Marie Reynouard, Pierre Bisch, André Coin

The Seismic Behavior of Reinforced Concrete Structural Walls: Experiments and Modeling

P. Kotronis, J. Mazars, X.H. Nguyen, N. Ile, J.M. Reynouard, P. Bisch and A. Coin

1 Introduction

Many European buildings are situated in seismic regions of low or moderate seismicity. Among these, a large part is not designed under parasismic regulations. Within this context the evaluation of the vulnerability of existing structures is an important issue. In the framework of the European Community Ecoleader programme, a seismic research project has been performed around shaking table tests on mock-ups representing parts of reinforced concrete buildings, the structure of which is based on structural walls. The program concerns two mock-ups: a Slovenian one and a French one (Fig. 1), the tests being performed at the laboratory LNEC in Lisbon.

This work is related to the analysis of the response of the French mock-up. The structure is characteristic of a typical building met in France designed according to the European regulation EC8-1 with the French appendix. It is composed of two parallel walls linked with a perpendicular one that has openings. All the walls are designed for the seismic level prescribed for a typical seismic region in France.

Two orthogonal directions of loading have been considered, X (parallel to the main walls) and Y (parallel to the wall connecting the main ones). Natural accelerograms at different levels have been used (PGA = from 0.3 g to 0.85 g for direction X and from 0.14 g to 0.50 g for direction Y) and various data have been collected from the different tests (strain on reinforcements, displacements, accelerations...). In order to follow the evolution of the stiffness, the apparent mode has been measured after each test.

Two kinds of modeling are performed hereafter: a simplified one using multifiber beams and a refined one, based on a 3D finite element description of the mock-up.

P. Kotronis (✉)
Laboratoire Sols, Solides, Structures-Risques (3S-R) INPG/UJF/CNRS and VOR research network, Grenoble, France
e-mail: Panagiotis.Kotronis@inpg.fr

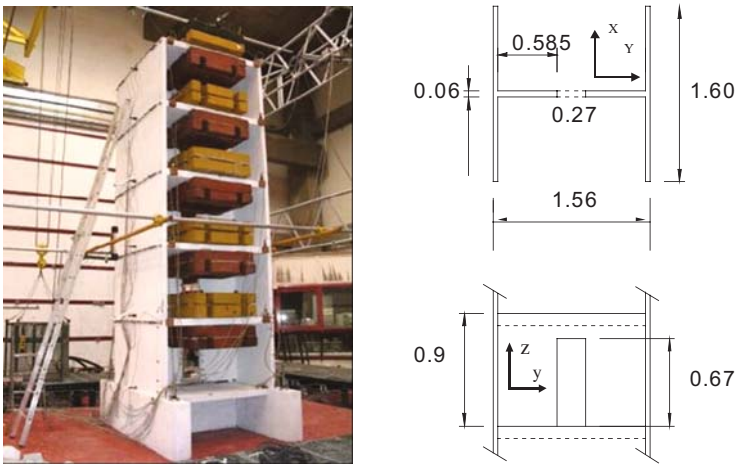

Fig. 1 Geometrical data of the French mock up (m)

Constitutive laws are based on damage mechanics and plasticity to describe cracking of concrete and the plastic behavior of steel. In order to reproduce correctly the behavior of the structure the stiffness of the shaking table have to be introduced in the models.

It will be shown that both models are able to describe the global behavior of the structure and qualitatively the distribution of damage. This conclusion confirms the results of previous works done on structural walls in France (Bisch and Coin 2007). For more detailed information on this test see (Bisch and Coin 2005), (Mazars et al. 2005), (Nguyen 2006).

2 Outline of the Test

Two kinds of artificially generated earthquake motions independent to each other, were applied in the X and Y directions. The sequences of tests are given in Table 1.

Table 1 Sequences of the tests

Tests	In plane (direct. X)	Out of plane (direct. Y)
T0	0.3 g	–
T1	–	0.14 g
T2	0.24 g	0.13 g
T3	0.45 g	0.27 g
T4	0.55 g	0.30 g
T5	0.74 g	0.36 g
T6	0.85 g	0.50 g

The main damages appeared at the base of the walls and one rebar has buckled (but not broken) for a signal closed to the design level (X PGA = 0.45 g – Y PGA = 0.27 g). For higher levels damage increased and at 0.85 g some rebars broke at the base of the walls where a large fracture appeared.

3 3D Model

To predict the inelastic seismic response with sufficient accuracy, due care has been given to create a detailed model of the specimen, taking into account the necessary geometric characteristics, construction details and boundary conditions. An example of the 3D finite element mesh used in the analyses is reported in Fig. 2. Due to the direction of the applied loading, in-plane as well as out-of-plane behavior of the walls need to be analyzed. A discrete modeling is adopted to represent the reinforcement through the use of two-node truss-bar elements. The structure is assumed fully restrained at all nodes along the base of the shear wall. During previous tests on CAMUS specimens (Bisch and Coin 2007), it was observed that the specimen oscillation have induced vertical and rocking displacements on the shacking table, leading to significant reductions of the

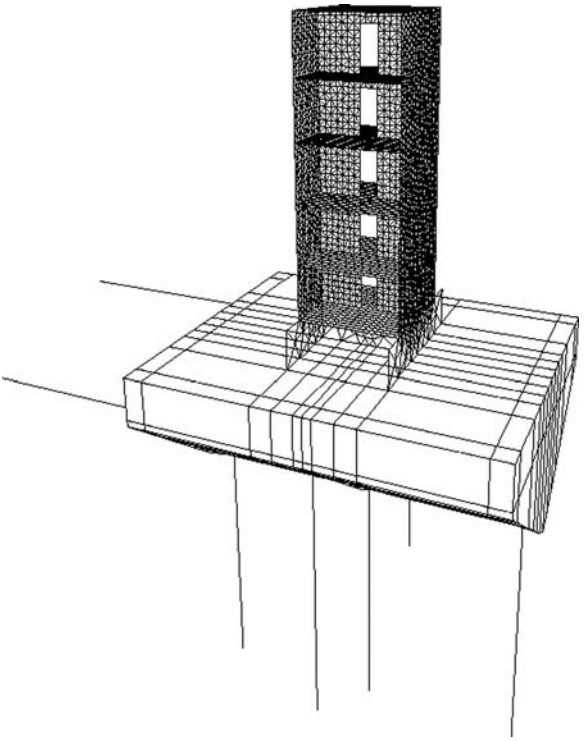

Fig. 2 3D finite element mesh of the specimen

corresponding natural frequencies. Therefore, the shaking table itself in terms of mass and its external supports in terms of stiffness have to be included into the numerical model. Perfect bond is assumed to exist between concrete and reinforcement. The possibility of non-linear material behavior is specified for all wall concrete and reinforcing bar-elements, while the behavior of the foundation and bracing system is considered as elastic. Assuming a 1% critical damping factor for the first and second vibration mode, the damping parameters a and b are calculated and used subsequently to form the Rayleigh damping matrix [C] = a[M] + b[K], M and K being the mass and stiffness matrix.

The concrete model used in analysis (Merabet and Reynouard 1999) adopts the concept of a smeared crack approach with a possible double cracking only at 90°. It is based upon the plasticity theory for uncracked concrete with isotropic hardening and associated flow rule. Two distinct criteria describe the failure surface: Nadai in compression and bi-compression and Rankine in tension. Hardening is isotropic and an associated flow rule is used. When the ultimate surface is reached in tension, a crack is created perpendicularly to the principal direction of maximum tensile stress, and its orientation is considered as fixed subsequently. Each direction is then processed independently by a cyclic uniaxial law (Fig. 3), and the stress tensor in the local co-ordinate system defined by the direction of the cracks is completed by the shear stress, elastically calculated with a reduced shear modulus to account for the effect of interface shear transfer: The model has been described in detail and verified elsewhere (Ile and Reynouard 2000), (Ile et al. 2002).

For steel, the cyclic behavior is described by the formulation proposed by Giuffré and Pinto and implemented by (Menegoto and Pinto 1973).

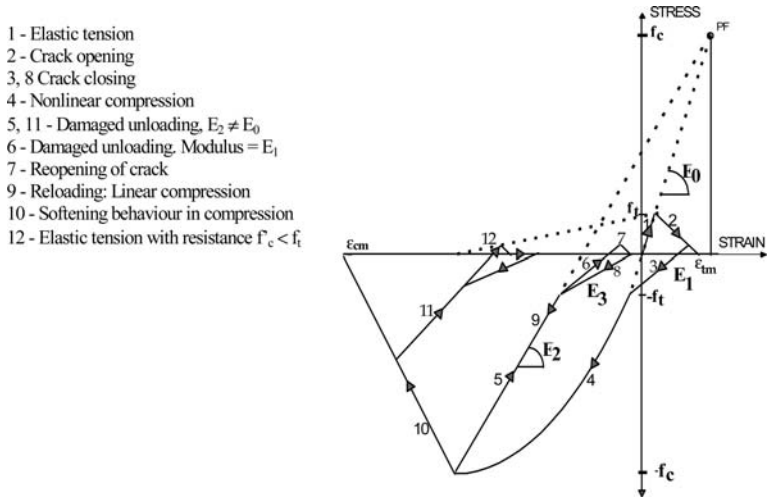

Fig. 3 Uniaxial cyclic law: point initially in tension

4 Simplified Model

Non-linear dynamic analysis of civil engineering structures requires large scale calculations. The necessity to perform parametrical studies led us to adopt a simplified approach in order to reduce the computational cost. The structure is modeled with beam elements to reduce the number of degrees of freedom of the problem. Using an Euler Bernoulli formulation the shear deformations are not modeled so we can use 1D versions of the non linear constitutive laws in the fibers (torsion is also kept linear). The multifiber beam used is the one implemented in the finite element code Aster (Ghavamian et al. 2002).

The finite element mesh is presented in Fig. 4. The additional masses and the weight load of each floor are concentrated at each storey. The Rayleigh damping coefficients have been adjusted to ensure a value of 1% on the two first modes.

The reinforcement steel is modeled with an isotropic cinematic hardening law. Constitutive model for concrete under cyclic loading ought to take into account some observed phenomena, such as decrease in material stiffness due to cracking, stiffness recovery which occurs at crack closure and inelastic strains concomitant to damage. To simulate this behavior we use a damage model with two scalar damage variables one for damage in tension and one for damage in compression (La Borderie 1991). Unilateral effect and stiffness recovery (damage deactivation) are also included. Inelastic strains are taken into account thanks to an isotropic tensor (Fig. 5).

5 Main Results

The modal analysis has been performed using both models in order to insure that the boundary conditions and the distribution of the masses are well represented. The stiffnesses of the springs below the shaking table are identified to feet the first eingenmodes measured on the virgin structure before the test.

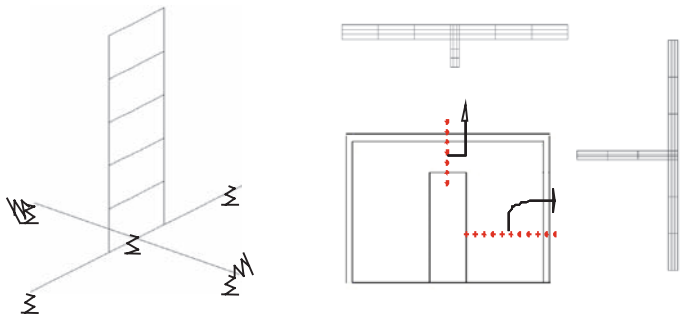

Fig. 4 Simplified finite element mesh of the specimen

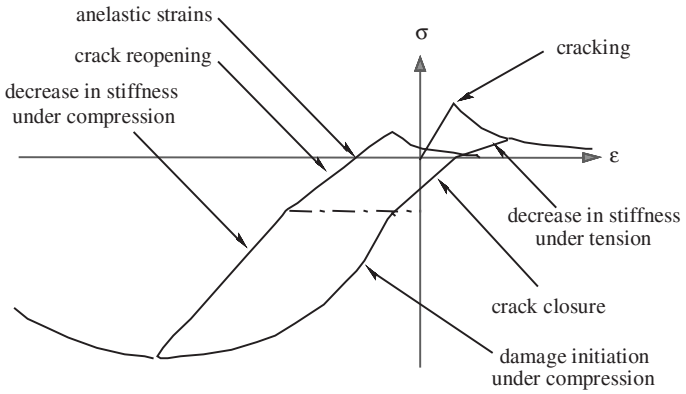

Fig. 5 1D cyclic response of the La Borderie model

Table 2 gives a comparison of the two approaches with the experimental results for the first three natural modes.

For the *3D model (refined model)* numerical analyses have been performed using the CAST3M finite element code. All the seismic signals applied to the specimen were considered in chronological order. The first comparisons presented in Figs. 6 and 7 concern the relative horizontal displacements in X and Y directions corresponding to the T5 (0.74 g) input motion, which caused significant damage to the specimen. The calculated response is generally under-

Table 2 Modal analysis

Model	In plane (direction X)	Out of plane (direction Y)	Torsion
Fiber model	4.54 Hz	 7.0 Hz	11.0 Hz
3D model	 4.5 Hz	 7.06 Hz	 9.9 Hz
Experiment	4.5 Hz	7.13 Hz	not known

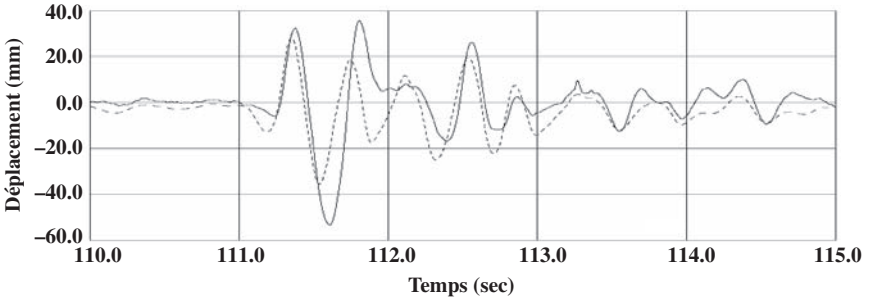

Fig. 6 Refined model, comparison between calculated and measured horizontal relative top – X displacement for T5 motion (0.74 g)

estimated in both directions and the correlation between analysis and experiment seems to be better for the X direction as compared to the Y direction. This may be due to the fact that the axial stiffness of the vertical rods supporting the shaking table may evolve during seismic response. It is difficult to take into account this aspect, when the variation of the axial stiffness of the rods is not known in advance. However, even if the numerical results do not match exactly the experimental ones, they give the opportunity to highlight some important characteristics of the structural behavior as described hereafter.

Local results as obtained from the dynamic analysis are presented in Fig. 8. This figure depicts the damage distribution corresponding to the maximum top displacement attained in the X direction for the T5 applied motion. The analysis results indicate that more damage is to be expected in the X walls as compared to the Y wall. They also show large compressive strains at one end of the X wall, indicating that concrete may fail in this location due to excessive strains. Actually, this seems to be in reasonable agreement with what was experimentally observed (Fig. 9): the wall extremities were heavily damaged in compression and steel bars buckled and have broken after that at this location.

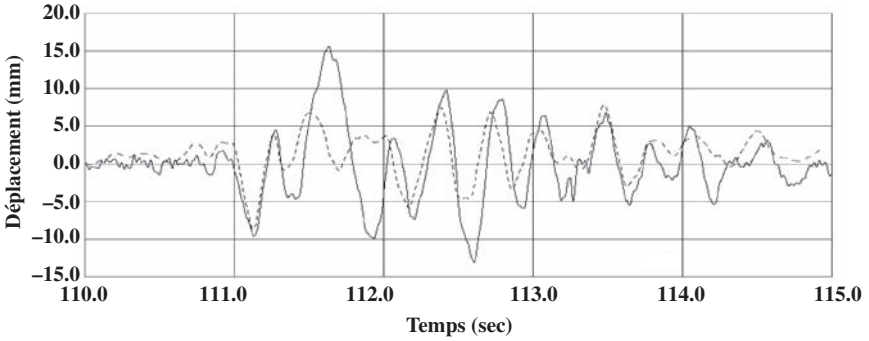

Fig. 7 Refined model, comparison between calculated and measured horizontal relative top – Y displacement for T5 motion (0.74 g)

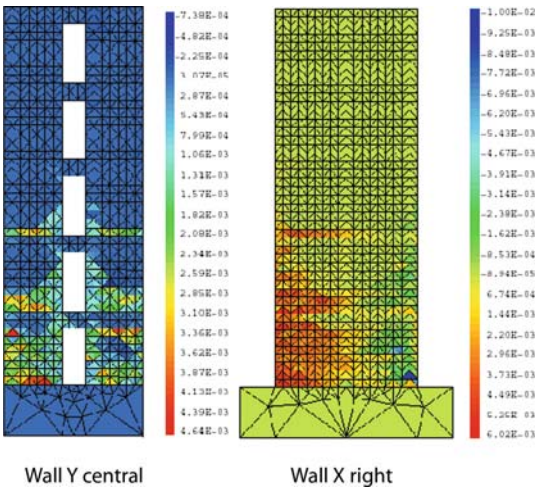

Fig. 8 Refined model, vertical concrete strain contours for T5 motion

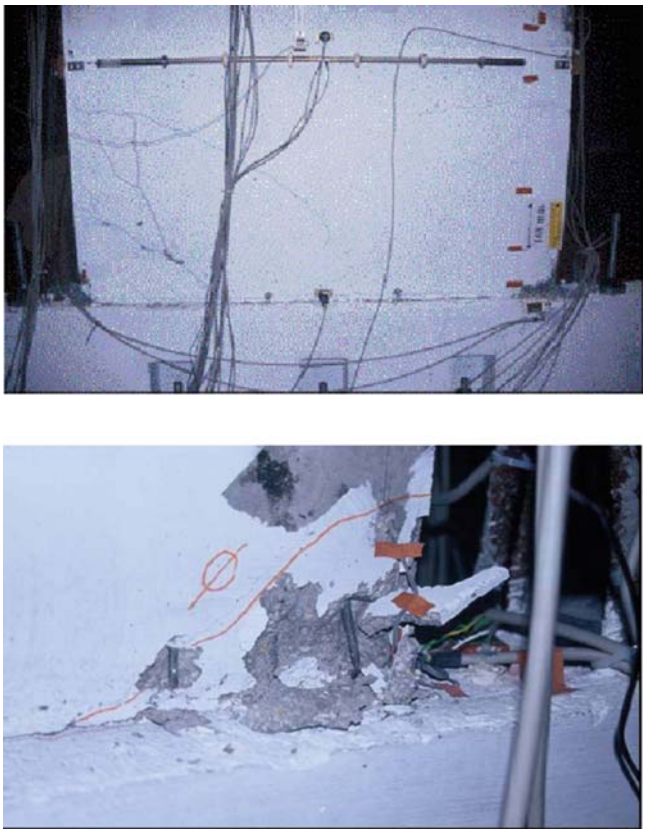

Fig. 9 Experimental damage pattern for T5 motion

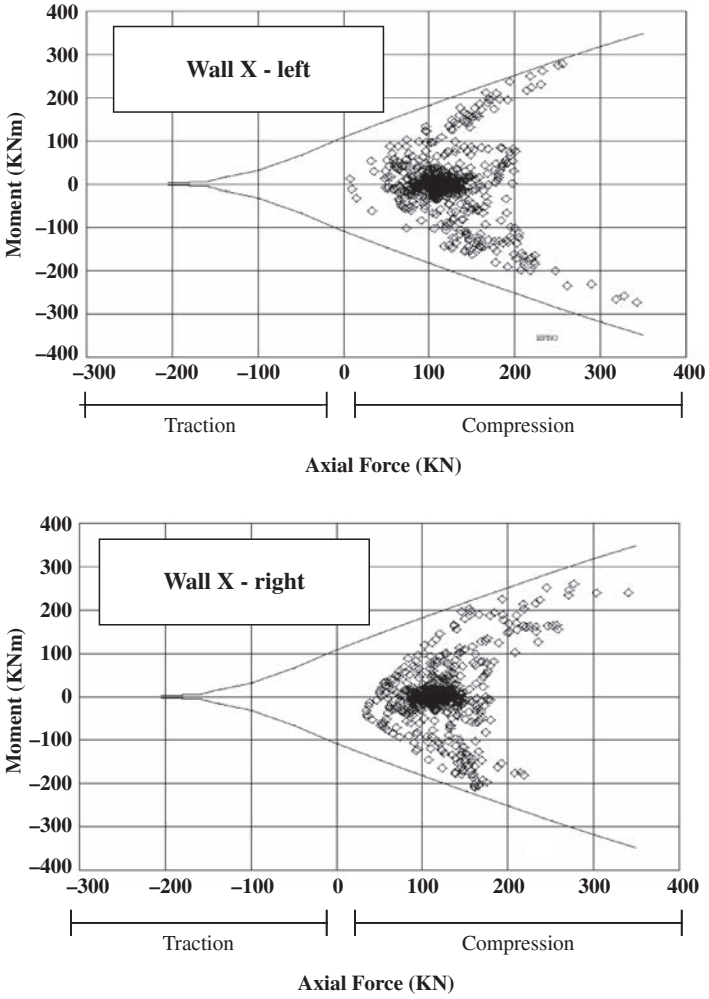

Fig. 10 Refined model, bending moment – axial force interaction diagrams and variation of bending moment and axial force at the base of the 1st storey (T5 motion)

Figure 10 presents numerical results in terms of bending moment – axial force interaction diagrams at the base of the 1st storey together with the variation of axial load and moment. This confirms the observed behavior and failure mode, since limit states tend to be obtained with high axial force values.

The numerical results of the *simplified model* are presented in Figs. 11 and 12. The time history of the calculated roof displacement is compared with the corresponding measured displacement for the T5 sequence. Simulation predicts satisfactory the maximum displacement for both sequences and there is no significant shifting between the curves.

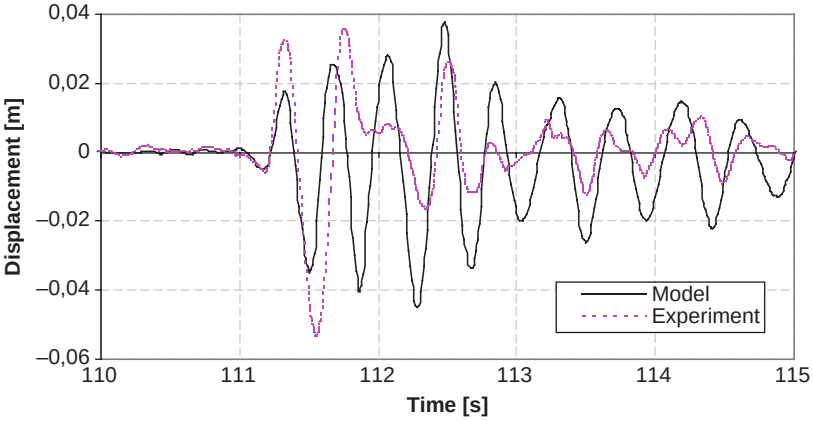

Fig. 11 Simplified model, comparison between calculated and measured horizontal relative top-X displacement for T5 motion (0.74 g)

The damage variable vary normally between 0 (non damaged section) and 1.0 (completely damaged section). By filtering their values between 0.95 and 1.0 we omit the micro-cracks and we have an image of the bigger cracks of the model. Figure 13 presents the damage pattern due to tension at the end of the calculation for the T5, where we can see that damage is concentrated at the base.

The evolution of the top displacement for T6 is presented in Figs. 14 and 15. Comparison of the distribution of damage and strains in the steels (Fig. 16) with the actual position of cracks (Figs. 17 and 18) shows again that the model is able to reproduce qualitatively the local behavior observed experimentally.

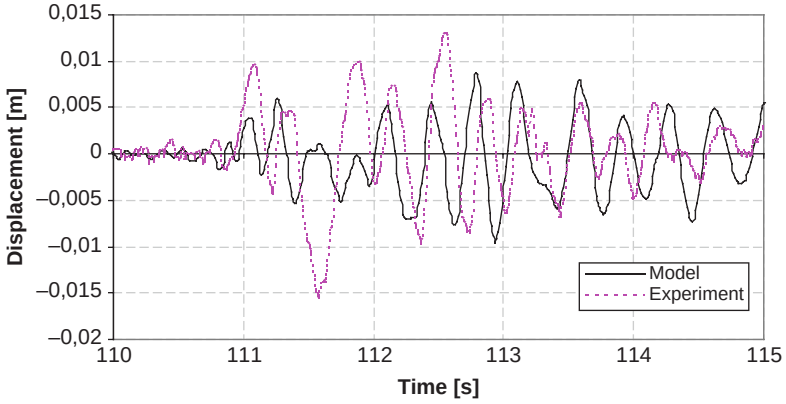

Fig. 12 Simplified model, comparison between calculated and measured horizontal relative top-Y displacement for T5 motion (0.74 g)

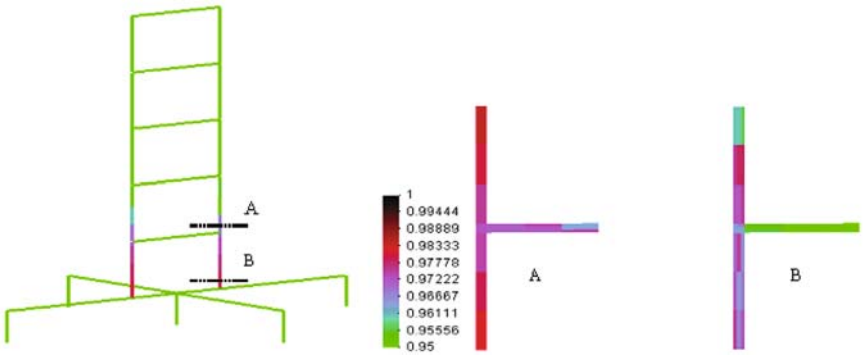

Fig. 13 Simplified model, state of damage for T5 motion

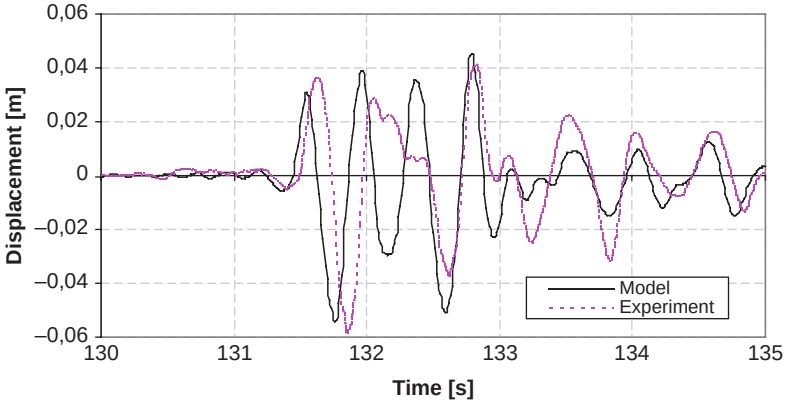

Fig. 14 Simplified model, comparison between calculated and measured horizontal relative top-X displacement for T6 motion (0.85 g)

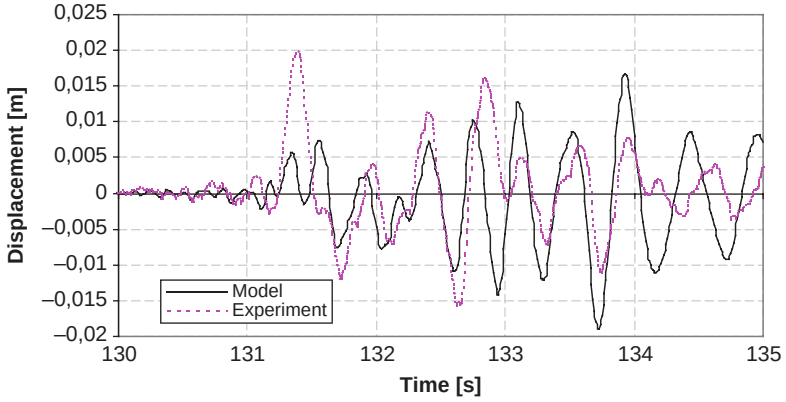

Fig. 15 Simplified model, comparison between calculated and measured horizontal relative top – Y displacement for T6 motion (0.85 g)

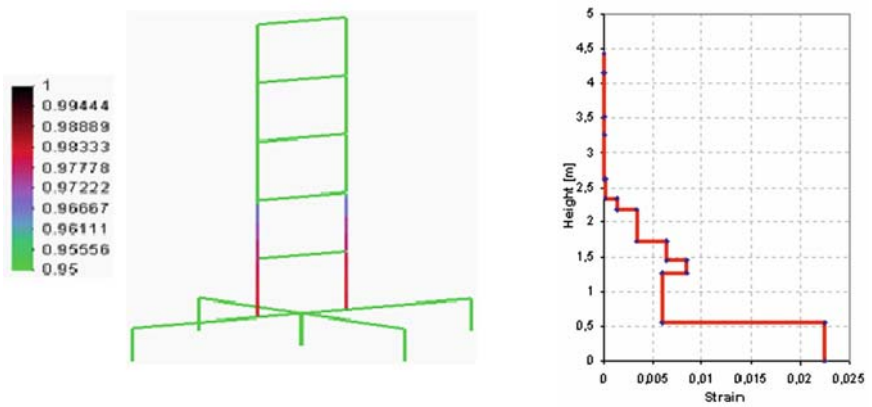

Fig. 16 Simplified model, state of damage in the structure and strain of reinforcement at the base of the wall X right for T6 motion

Main damages are again located at the base of the specimen. Furthermore, as shown in Fig. 16, the simplified model provides strains exceeding 2%, a limit corresponding to the ultimate strain of the reinforcement used in the experiment.

Fig. 17 Experimental damage pattern for T6 motion

Fig. 18 Broken steel at the base of the wall X right for T6 motion

6 Conclusions

As demonstrated by the results presented in the paper both models were able to reproduce with good approximation the global response of the structure and qualitatively the distribution of damage. A refined 3D model allows obtaining detailed information about the behavior of the specimen under complex loading conditions whereas a simplified approach helps reducing computational cost.

The works highlights once again the importance of the axial force variation and its influence on the failure mode to be expected in the case of lightly reinforced walls. Based on the results obtained in this study, it appears now possible to use these models to investigate numerically the behavior of a wider variety of configurations that is practically impossible to study experimentally.

References

Bisch P, Coin A (2005) Seismic behaviour of slightly reinforcement walls. International Conference 250th anniversary of the 1775 Lisbon earthquake, Lisbon Portugal 1–4 November, pp. 518–522

Bisch P, Coin A (2007) Seismic Behaviour of Slightly Reinforced Concrete Walls: Experiments and Theoretical Conclusions, Bulletin of Earthquake Engineering, Vol. 5, No. 1, February

Ghavamian S, Davenne L, Gatuingt F (2002) Elément de poutre multifibre (droite). Fascicule R3.08 – Document Code Aster

Ile N, Reynouard JM (2000) Non-linear analysis of reinforced concrete shear wall under earthquake loading, Journal of Earthquake Engineering, Vol. 4, No. 2, pp. 183–213

Ile N, Reynouard JM, Georgin JF (2002) Non-linear Response and Modelling of RC Walls Subjected to Seismic Loading, ISET Journal of Earthquake Technology, Vol. 39, No. 1–2, March–June, 20p

La Borderie CL (1991) Phénomènes unilatéraux dans un matériau endommageable: modélisation et application à l'analyse des structures en béton. PhD thesis, Université Paris 6

Mazars J, Nguyen XH, Kotronis P, Ile N, Reynourd JM (2005) Etude sur le fonctionnement sismique de structures à murs à cellules contreventées, Contrat No.04MGC 5 07, Org. Rapport final (Novembre) – Contrat DRAST/ Mission Génie Civil (http://hal.archives-ouvertes.fr/hal-00121989)

Menegoto M, Pinto P (1973) Method of analysis of cyclically loaded reinforced concrete plane frames including changes in geometry and non-elastic behaviour of elements under combined normal force and bending, IABSE Symposium on resistance and ultimate deformability of structures acted on by well-defined repeated loads, Final report, Lisbon, 328p

Merabet O, Reynouard JM (1999) Formulation d'un modèle elasto-plastique fissurable pour le béton sous chargement cyclique. Contract Study EDF/DER, Final Report, No.1/943/002, URGC-Structures, National Institute for Applied Sciences, Lyon, France, 84p

Nguyen XH (2006) Vulnérabilité des structures en béton armé à voiles porteurs: expérimentation et modélisation, PhD thesis, Institut National Polytechnique de Grenoble, INPG (http://tel.archives-ouvertes.fr/tel-00087712)